Bioorganic & Medicinal Chemistry 18 (2010) 2107–2114

Contents lists available at ScienceDirect

Bioorganic & Medicinal Chemistry

journal homepage: www.elsevier.com/locate/bmc

Design and synthesis of novel series of pyrrole based chemotypes and their evaluation as selective aldose reductase inhibitors. A case of bioisosterism between a carboxylic acid moiety and that of a tetrazole

Kyriaki Pegklidou [a], Catherine Koukoulitsa [b], Ioannis Nicolaou [a,*], Vassilis J. Demopoulos [a]

[a] Department of Pharmaceutical Chemistry, School of Pharmacy, Aristotle University of Thessaloniki, Thessaloniki 54124, Greece
[b] Department of Chemistry, University of Athens, Zographou 15784, Greece

ARTICLE INFO

Article history:
Received 15 October 2009
Revised 2 February 2010
Accepted 5 February 2010
Available online 11 February 2010

Keywords:
Antidiabetic aldose reductase inhibitors
Antioxidant activity
Nonclassical bioisosterism
Selectivity

ABSTRACT

Pyrrolyl-propionic and butyric-acid derivatives **1** and **2** were synthesized in order to study the effect of the variation of the methylene chain in comparison to the previously reported pyrrolyl-acetic acid compound **I**, which was found as potent aldose reductase inhibitor, while the pyrrolyl-tetrazole derivatives **3**–**5** were prepared as a non-classical bioisosteres of a carboxylic acid moiety. Also, pyrrolyl-tetrazole isomers **6** and **7** without an alkyl chain between the two aromatic rings were synthesized. The in vitro aldose reductase inhibitory activity of the prepared **1**–**7** compounds were estimated and compared with that of the initial compound (**I**). Overall, the data indicate that the presented chemotypes **6** and **7** are a promising lead compounds for the development of selective aldose reductase inhibitors, aiming to the long-term complications of diabetes mellitus.

1. Introduction

Diabetes mellitus is a metabolic disease in which the body's ability to regulate blood glucose levels goes awry, either from defects in the secretion or in the activity of the hormone insulin. Today, the worldwide prevalence of diabetes is taking pandemic dimensions. In 2003, 194 million people globally, ranging in age from 20 to 79 years, were suffering from diabetes. By 2025, this number is projected to increase to 333 million.[1]

People with diabetes are vulnerable to late onset complications such as retinopathy, nephropathy and neuropathy that are largely responsible for the morbidity and mortality observed in patients.[2,3] The direct economic cost of diabetes is about 10 percent of the total health care budget, and approximately 90 percent of the total direct cost is needed for the treatment of the devastating diabetic complications.[4,5] The chronic complications of the disease are associated with the duration and the degree of hyperglycemia. It has been demonstrated that the more severe and sustained the degree of hyperglycemia, the more likely it is that the chronic complications of diabetes will develop.[6]

Under hyperglycemic conditions, there is an increased flux through the polyol pathway, accounting for greater than 30% of glucose metabolism.[7] Aldose reductase (ALR2; AR; EC 1.1.1.21) which is the first enzyme of the polyol metabolic pathway that converts glucose to sorbitol, was first found to be implicated in the etiolology of the long-term diabetic complications. Its inhibition by aldose reductase inhibitors (ARIs) has been gaining attention over the last decades from the pharmaceutical community as a promising pharmacotherapeutic target.[8]

Recently, in our laboratory, effective ARIs have been synthesized, which are derivatives of the pyrrolyl-acetic acid moiety (**I**).[9] In the present work, the elongation of the methylene chain as well as the replacement of the carboxylic acid moiety with that of the non-classical bioisosteric heterocyclic ring of tetrazole and their effect on aldose reductase activity were studied. The main advantage of the tetrazole derivatives in comparison to those of the carboxylic acid ones is that tetrazoles escape most of the phase II biotransformation of carboxylic acids.[10] In addition, although tetrazole derivatives are ionized in blood pH in a similar way to that of carboxylic acids, they are 10 times more lipophilic.[11] This increase in the lipophilicity could be relevant to their increased permeability through biomembranes.[11] Thus, a series of pyrrolyl-acids **1** and **2** and pyrrolyl-tetrazole **3**–**5** derivatives as well as pyrrolyl-tetrazole isomers **6** and **7** without an alkyl chain between the two heteroaromatic rings (Fig. 1) were designed synthesized and tested for their potential to inhibit the enzyme ALR2. In addition, the inhibitory activity of compounds **1**–**7** towards aldehyde reductase (ALR1) was studied, in order to define the selectivity between these two enzymes with similar amino acid sequence (65%).[12,13]

Furthermore, for selected more active ones the antioxidant potential was assessed in a homogeneous 2,2-diphenyl-1-pic-

* Corresponding author. Tel.: +30 2310 998670; fax: +30 2310 997852.
E-mail address: inikolao@pharm.auth.gr (I. Nicolaou).

0968-0896/$ - see front matter © 2010 Elsevier Ltd. All rights reserved.
doi:10.1016/j.bmc.2010.02.010

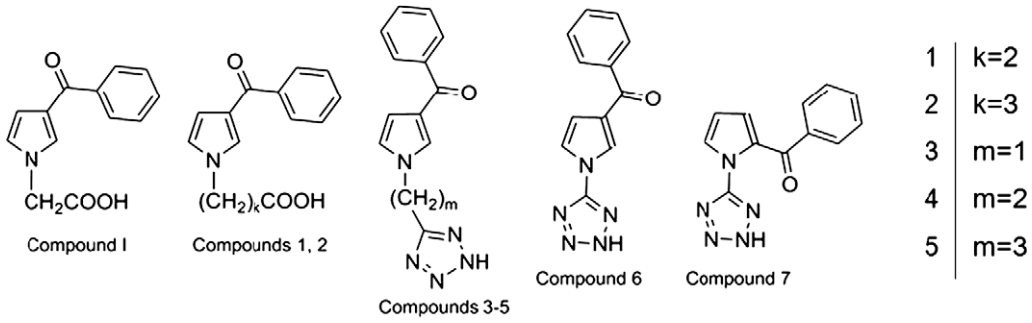

Figure 1. Structures of pyrrolyl-acids and pyrrolyl-tetrazole derivatives.

rylhydrazyl (DPPH) assay system,[14] as well as in a heterogeneous unilamellar L-α-phosphatidylcholine dioleoyl (DOPC) liposomes' assay system.[14] Oxidative stress is well-established as an important biochemical factor implicated in the long-term complications of diabetes mellitus.[15,16]

2. Results and discussion

2.1. Chemistry

The preparation of the compounds **1** and **2** was based on the reported methodology[17,9] and it is shown in Scheme 1. The synthesis of compounds **3–5** was a two-step procedure (Scheme 1). The first step included the formation of the intermediates pyrrolyl-nitrile derivatives via a nucleophilic substitution under a phase transfer catalysis for the preparation of compounds **3** and **5** and via a Michael reaction for compound **4**.[18] The second step included the conversion of pyrrolyl-nitrile derivatives to the final pyrrolyl-tetrazole compounds using trimethylsilyl azide in the presence of a catalytic amount of dibutyltin oxide in refluxing toluene.[19] A number of different conditions was studied for the preparation of the intermediates pyrrolyl-nitrile derivatives **3i** and **5i**, using benzyltributylammonium chloride (BTAC) or *tris*-[2-(2-methoxyethoxy)ethyl]amine (TDA-1) as phase transfer catalysts in tetrahydrofuran (THF) or toluene, respectively. Best results were obtained with BTAC in THF as solvent. The synthesis of the isomeric compounds **6** and **7** was based on a Friedel–Crafts aroylation of 1-(1*H*-pyrrol-1-yl)-1*H*-tetrazole (**6i**), which was synthesized from 5-amino-tetrazole by a modified Clauson–Kaas reaction.[9] The Friedel–Crafts aroylation was performed according to Nicolaou and Demopoulos[20] using nitromethane as a cosolvent. Both compounds **6** and **7** were isolated from the above reaction.

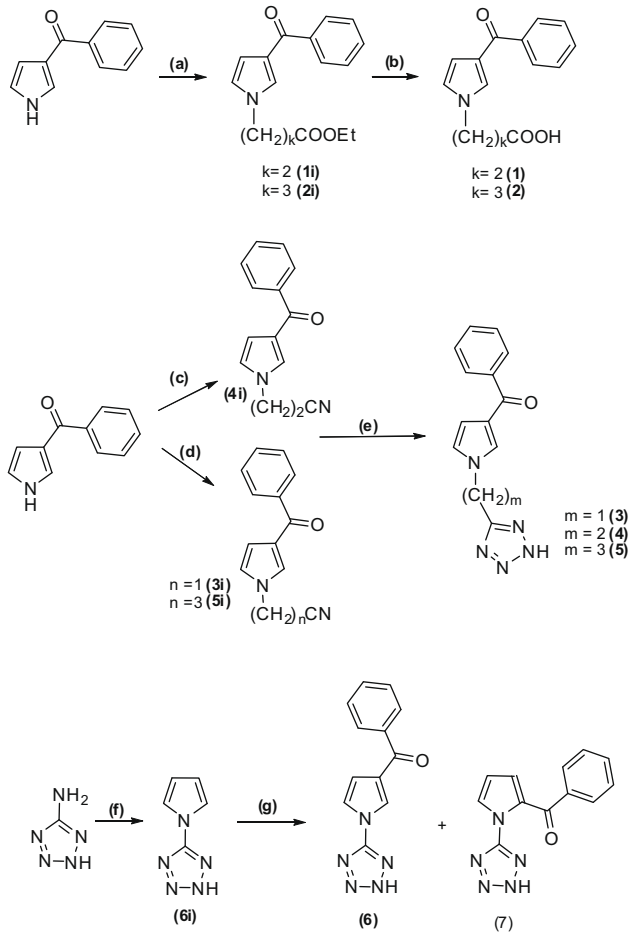

Scheme 1. Reagents and conditions: (a) ethyl bromopropanate or ethyl bromobutanate, NaH, TDA-1, toluene; (b) 5% aq. NaOH, dioxane; (c) acrylonitrile, Triton B; (d) 2-bromoacetonitrile or 4-bromobutanenitrile, NaH, BTAC, THF; (e) Me_3SiN_3, $nBu_2Sn{=}O$, toluene; (f) 2,5-bimethoxy-tetrahydrofuran, 4-chloropyridine hydrochloride, 1,4-dioxane; (g) $AlCl_3/CH_3NO_2$, PhCOCl, CH_2Cl_2.

2.2. In vitro and in silico results

2.2.1. Aldose reductase inhibitory activity

The synthesized compounds **1–7** were evaluated in vitro for their ability to inhibit partially purified rat lens AR. It has been shown that there is an approximately 85% sequence similarity between rat lens and human ALR2, while the proposed active sites of both enzymes are identical.[21] The performed assay was based on a spectrometric measurement, which is proven to be a reliable method,[22] with DL-glyceraldehyde as the substrate and NADPH as the cofactor. Sorbinil was used as a positive control. Inhibitor IC_{50} values were determined for those compounds displaying greater than 50% percent inhibition at the high concentration of 10^{-4} M. Results

Table 1
Aldose reductase inhibitory activity data

Compound	% Inhibition (±SD[a]) 10^{-4} M	
		IC_{50} (±SD[a]) μM
1		9.7 (±0.15)
2		6.04 (±0.11)
3	40 (±4.1)	
4	6 (±0.4)	
5	41(±0.39)	
6		18.0 (±1.49)
7		20.0 (±0.96)
I		1.97 (±0.03)[b]
Sorbinil		0.25 (±0.006)[c]

[a] $n = 3$
[b] Reported data by Nicolaou and Demopoulos.[9]
[c] Reported IC_{50}: 0.07 μM by Kador and Sharpless.[23]

are presented in Table 1 and compared with compound **I**, which has been previously shown that is an effective ARI.[17,9]

It was found that pyrrolyl-propionic or butyric-acid derivatives **1** and **2** have IC_{50} values a little higher than their acetate counterpart (compound **I**). This is in accordance to the well-established pharmacophore role of the acetic acid functionality in the majority of the carboxylate ARIs.[24] It is also, worth noting that the butyrate derivative **2** is more potent than the propionate derivative **1**. In a similar example Sun et al noticed that a number of indolobutanoic acid derivatives have been shown to be active in submicromolar range as ARIs.[25] The replacement of the carboxylic acid moiety with that of the bioisosteric heteroaromatic ring of tetrazole in cases of compounds **3** and **5**, dramatically reduce the inhibitory activity, while compound **4** was found to be completely inactive at the same concentration. This is also in agreement with that previously referred about the propionate counterpart. On the other hand, the lack of the methylene chain between pyrrole and tetrazole aromatic rings in compounds **6** and **7** improves noticeably the total inhibition, in comparison to tetrazole derivatives which have an alkyl chain. Inspection of low energy conformations of all tetrazole derivatives reveals that the two heterocyclic aromatic rings of compounds **3**–**5** are not in the same plane as they are, in compounds **6** and **7** (Fig. 2). This is also in accordance with that previously reported by Nicolaou and Demopoulos.[9]

In order to shed light on their interactions in the active site of ALR2, docking simulations were performed. The human aldose reductase holoenzyme complexed with IDD 594 (PDB entry 1US0) was selected, as it was determined at the highest resolution (0.66 Å) among all the available structures. The docking simulations in the active site of ALR2 were performed by the docking GLUE program, which has been shown to successfully reproduce experimentally observed binding modes in terms of rmsd (root-mean squared deviation). The crystallographic structure of IDD 594 was docked into ALR2 with GLUE provided excellent result as shown in our previous work.[26]

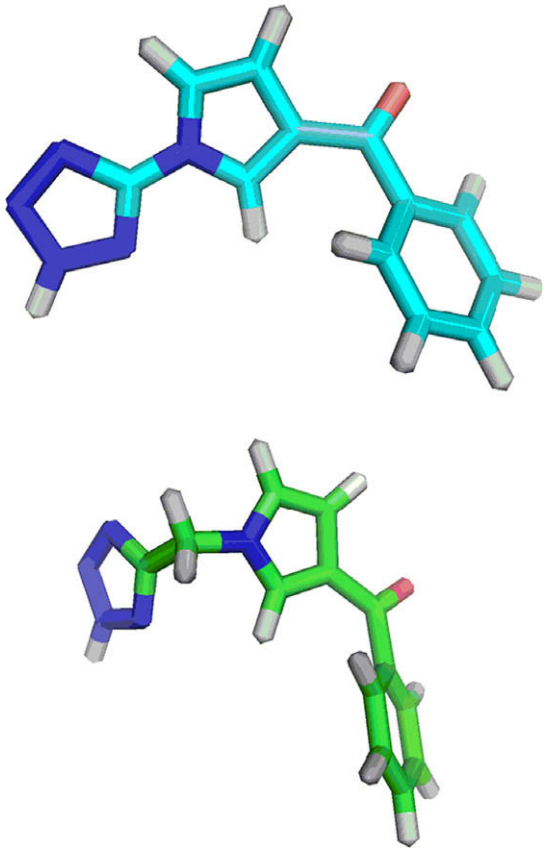

Figure 2. Representative low energy conformations of tetrazole-derivative **3** (down) versus tetrazole-derivative **6** (up).

It is observed that the most active compound (**6**) exhibits the higher binding energy (−21.65 Kcal/mol). Compound **7** possess similar binding energy (−21.14 Kcal/mol), while the inactive compound **3** exhibits the lower binding energy (−15.76 Kcal/mol). As illustrated in Figure 3a–c, the compounds were placed in the same location as IDD 594 in the crystal structure. In particular, the tetrazole moiety of compounds **6** and **7** is anchored in the anionic binding site forming polar interactions with Tyr48 and electrostatic interactions with the positively charged nicotinamide ring of $NADP^+$. Compound **7** forms polar interactions also between the phenyl oxygen and Trp111. Further stabilization of the molecules is attributed to the aromatic interactions of the phenyl ring with Trp79, Trp111, Trp219 and Van der Waals interactions between phenyl ring and residues Phe122, and Leu300. Compound **3** entered the anionic binding site with the phenyl ring, and can not establish strong interactions with the key aminoacid residues and $NADP^+$. The results from the docking calculations are in consistence with the lower estimated binding energy and the observed inactivity of compound **3** against aldose reductase.

In Figure 3d is presented the superimposition of the docked compounds **6** and **7** and IDD594 in the active site of ALR2. It should be noticed that the phenyl ring entered in the specificity pocket localized between Phe122, Trp111, Leu300, and Ala299 as IDD594, suggesting a selectivity for aldose versus aldehyde reductase.

2.2.2. Aldehyde reductase inhibitory activity

An important feature of pharmacologically applicable ARIs is their selectivity of action. The co-inhibition of structurally related physiological oxidoreductases might have unwanted side effects. In the present study, the target compounds **1–7** and **I** were also tested for their selectivity. In testing for selectivity we used the enzyme aldehyde reductase (ALR1, EC 1.1.1.1.2). The assay was based on a spectrometric measurement, using D-glucuronate as a substrate in the presence of NADPH as a cofactor.[27] ALR1 and ALR2 share a high degree of sequence (~65%) and structural homology.[28] ALR1 is one of the significant enzymes for the reduction of many aldehydes, counteraction and excretion of drugs, reduction of 3-deoxyglucosone (3-DG), which is an intermediate for advanced glycation end-products (AGEs), and metabolism of methylglyoxal.[29] Valproic acid was used as a positive control. Results are shown in Table 2. As it could be seen, compounds **1**, **2**, **6**, **7** and **I** have high selectivity for aldose versus aldehyde reductase since they possess very low inhibitory activity towards ALR1 at the high concentration of 10^{-4} M.

2.2.3. DPPH scavenging activity

In this part of our work, three of the most active and selective pyrrolyl ARIs **I**, **6** and **7** were assessed in vitro for the radical scavenging potential of them, by using the model reaction with the stable free radical of 2,2-diphenyl-1-picrylhydrazyl (DPPH). In this homogeneous system of the ethanol solution of DPPH, antioxidant activity stems from an intrinsic chemical reactivity towards radicals. DPPH, as a weak hydrogen radical atom abstractor, could be considered as a good kinetic model for peroxyl $ROO^{\cdot}$ radicals.[30] Results indicated a slight antioxidant potential at the equimolar concentrations (0.2 mM) of the tested compounds and DPPH (~10% scavenging activity). Trolox which was used as a reference compound had shown 98% scavenging activity at the same concentration.

2.2.4. Lipid peroxidation inhibition

In membranes, the relative antioxidant reactivity is probably different from a homogeneous system since it is determined by additional factors, such as the location of the antioxidant and rad-

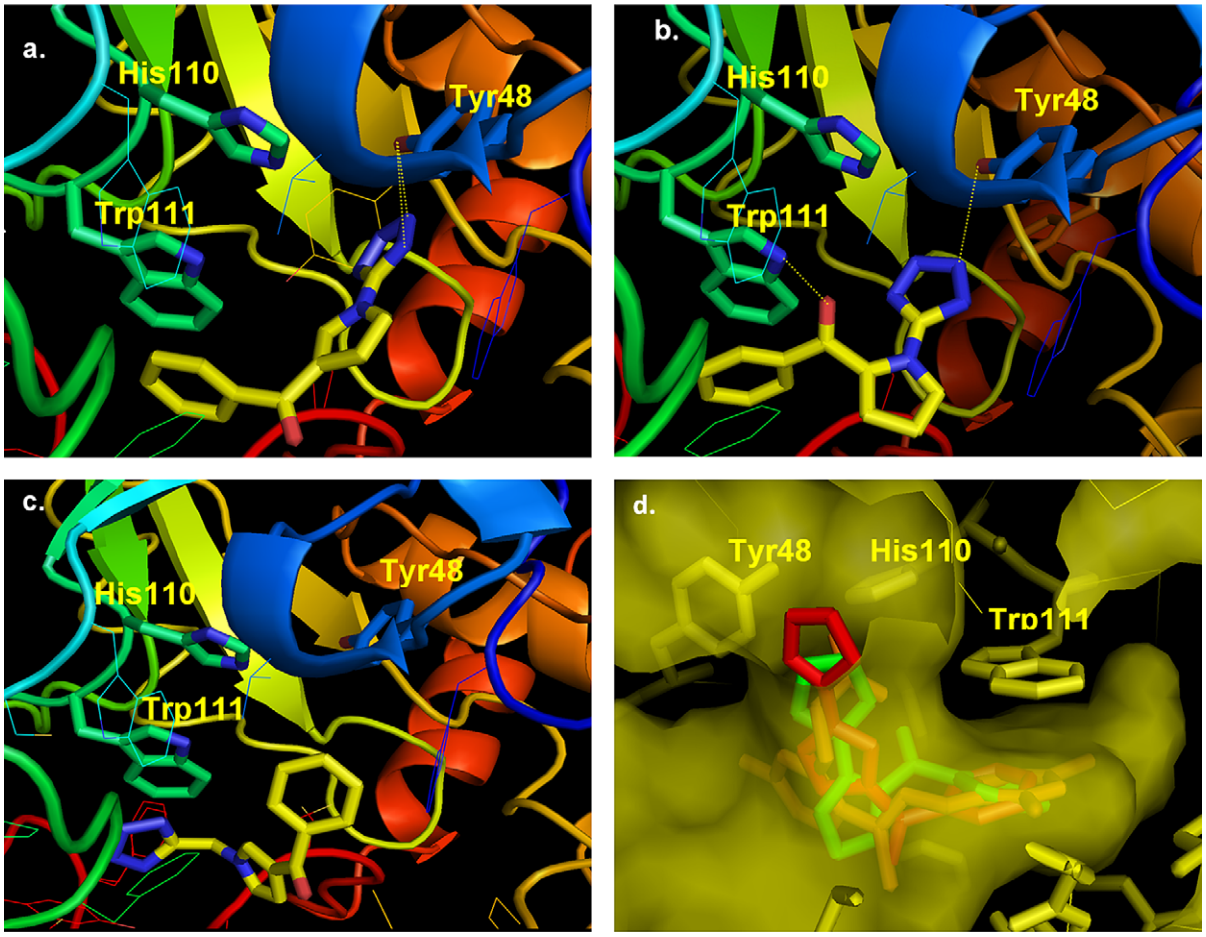

Figure 3. Docked orientations of (a) compound **6**, (b) compound **7**, and (c) compound **3**, with additional depiction of the key aminoacids of ALR2 active site. Polar interactions are shown as dotted lines; (d) Superimposition of the docked compounds **6** (red), **7** (green), and **IDD594** (orange) in the active site of ALR2.

Table 2
Aldehyde reductase inhibitory activity data

Compound	% Inhibition (±SD)[a] 10^{-4} M
1	20 (±6.5)
2	22 (±1.53)
3	23 (±2.52)
4	41 (±0.58)
5	35 (±2.52)
6	18 (±1.75)
7	18 (±1.00)
I	34 (±3.51)
Valproic acid	IC_{50}[b]: 50.1 (±3.0) μM

[a] $n = 3$.
[b] Reported IC_{50}: 56.1 (±2.7) by Stefek and co-workers.[14]

icals and is ruled predominantly by the partition ratios between water and lipophilic compartments. As an indicative heterogeneous assay, the antioxidant inhibitory efficiency of compounds **I**, **6** and **7** was evaluated in the system of unilamellar DOPC liposomes oxidatively stressed by peroxyl radical generated in the aqueous phase by thermal decomposition of the hydrophilic azo initiator 2,2-azobis(2-amidinopropane) hydrochloride (AAPH). Results indicated a weak antioxidant potential of compounds (IC_{50} >300 μM). Trolox in an identical assay was used as the positive control (IC_{50} = 93.5 μM).[31]

2.2.5. 'Drug-likeness'

The 'drug-likeness' of the novel aldose reductase inhibitors was assessed on the basis of their structural properties by applying the Lipinski's 'rule of five', and moreover the topological polar surface area (TPSA) as additional molecular descriptor[32–34] (Table 3). For all the drug candidates studied, none of the criteria was violated, thus predicting their good oral bioavailability.

3. Conclusion

Pyrrolyl-acids **1**, **2** and **I** as well as pyrrolyl-tetrazoles **6** and **7** have been found to be promising selective aldose reductase inhibitors. It should be noted at this point that the selective activity for aldose versus aldehyde reductase is considered as a great advantage for a compound because of reduction of the risk for toxic

Table 3
Drug-likeness of the synthesized compounds

Compound	MW (<500)	NH/OH (<5)	N/O (<10)	Clog *P* (<5)	TPSA (Å^2)
1	243.28	1	4	2.04	59.30
2	257.31	1	4	2.40	59.30
3	253.29	1	6	0.96	76.46
4	267.32	1	6	1.06	76.46
5	281.35	1	6	1.44	76.46
6	239.26	1	6	1.07	76.46
7	239.26	1	6	1.07	76.46

MW, molecular weight; OH/NH, number of H-bond donors; O/N, number of H-bond acceptors; Clog *P* v. 4.0 (Biobyte), based on Leo-Hansch fragmental system (Clog *P*); TPSA, topological polar surface area calculated by Pallas v.3.3.2.4 (CompuDrug Chemistry Ltd.

effects. Furthermore, properties implicit to 'drug-likeness', inferred from simple molecular descriptors, rendered novel aldose reductase inhibitors potential drugs with expected good bioavailability and with a prospect of further optimization. Additionally, compounds **6** and **7** as tetrazole-derivatives might have a better pharmacokinetic profile than pyrrolyl-acids derivatives. Thus, we propose that compounds **6** and **7** could comprise the basis for the design of novel chemotypes, as pharmacotherapeutic agents for the treatment of the long-term diabetic complications.

4. Experimental section

4.1. General notes

Unless otherwise stated, all commercial reagents were available from Aldrich, Sigma or Fluka. Melting points were determined in open glass capillaries using a Mel-TempII apparatus. UV spectra were recorded either on a Perkin–Elmer 554 or on a Hitachi U-2001 spectrophotometer. IR spectra were obtained on a Shimadzu spectrophotometer, and ^{1}H NMR spectra on a Bruker AW-80 spectrometer with internal TMS standard. LC–MS/MS spectra were obtained using an Acquity Waters UPLC–MS/MS (Triple quandropole) system, while a Shimadgu 2010-EV LC/MS was used for obtaining LC/MS spectra. Elemental analyses were performed in School of Chemistry, Department of Organic Chemistry of Aristotle University. Statistical analyses were performed using SPSS v.12.0.

4.2. Chemistry

4.2.1. General procedure for the preparation of the ethyl propanoic and ethyl butanoic acid esters derivatives (1i and 2i)

To a cold (ice bath) stirred and under a nitrogen atmosphere mixture of phenyl(1*H*-pyrrol-3-yl)methanone (12.86 mmol), ethyl bromopropanate or ethyl bromobutanate (19.29 mmol), respectively, and TDA-1 (2.06 mmol) in toluene (200 mL) was added NaH (60% dispersion in mineral oil) (19.29 mmol). The resulting mixture was stirred at room temperature for 24 h. After this period, it was poured into a stirred, ice cold mixture of Et_2O (100 mL) and 5% HCl (100 mL). The two phases were separated, and the aqueous phase was extracted with Et_2O (2 × 100 mL). The combined organic extracts were washed with 10% $NaHCO_3$ and saturated brine and dried over anhydrous sodium sulfate. The solvents were evaporated under reduced pressure and the residue was flashed chromatographed with petroleum ether/EtOAc 4:1 to afford **1i** and **2i** (yellow oils) and used without further purification for the next step of the reaction.

4.2.2. General procedure for the preparation of the propanoic and butanoic acid derivatives (1 and 2)

A mixture of **1i** or **2i** (4.61 mmol), dioxane (80 mL), and 5% NaOH (80 mL) were stirred at room temperature for 1 h. After this period, it was concentrated to half of its volume, H_20 (80 mL) was added, and the mixture was cooled (ice bath) and acidified with concentrated HCl. The formed precipitate was collected and the filtrate was extracted with CH_2Cl_2 (2 × 50 mL). The organic phase was washed with saturated brine and evaporated. The residue was combined with the precipitate and recrystallized from toluene/petroleum ether.

4.2.2.1. 3-(3-Benzoyl-1*H*-pyrrol-1-yl)propanoic acid (1). Yield 85%, mp 143–144 °C, IR (Nujol): 1731, 1540 cm^{-1}, ^{1}H NMR ($CDCl_3$/DMSO-d_6): δ 2.80 (t, 2H, CH_2CO), 4.20 (t, 2H, N–CH_2), 6.60–6.82 (m, 2H, pyrrolyl-4,5*H*), 7.25–7.60 (m, 3H, phenyl-*H*), 7.70–8.00 (m, 3H, phenyl-*H* and pyrrolyl-2*H*), 9.30 (br s, 1H, COO*H*). Anal. Calcd for $C_{14}H_{13}O_3N$: C, 69.12; H, 5.39; N, 5.76. Found: C, 69.13; H, 5.39; N, 5.72.

4.2.2.2. 4-(3-Benzoyl-1*H*-pyrrol-1-yl)butanoic acid (2). Yield 79%, mp 106 °C, IR (Nujol): 1730, 1540 cm^{-1}, ^{1}H NMR ($CDCl_3$/DMSO-d_6): δ 1.92–2.42 (m, 4H, CH_2CH_2CO), 4.10 (t, 2H, N–CH_2), 6.60–6.82 (m, 2H, pyrrolyl-4,5*H*), 7.20–7.60 (m, 3H, phenyl-*H*), 7.70–8.00 (m, 3H, phenyl-*H* and pyrrolyl-2*H*), 9.30 (br s, 1H, COO*H*). Anal. Calcd for $C_{15}H_{15}O_3N$: C, 70.02; H, 5.88; N, 5.44. Found: C, 70.07; H, 5.83; N, 5.37.

4.2.3. General procedure for the preparation of 2-(3-benzoyl-1*H*-pyrrol-1-yl)acetonitrile (3i) and 4-(3-benzoyl-1*H*-pyrrol-1-yl)butanenitrile (5i)

To a cold (ice bath) stirred under a nitrogen atmosphere mixture of phenyl(1*H*-pyrrol-3-yl)methanone (2.92 mmol), 2-bromoacetonitrile or 4-bromobutanenitrile (2.92 mmol), respectively, and a small quantity of benzyltributylammonium chloride (BTAC) (0.292 mmol) in tetrahydrofuran (30 mL), was added NaH (60% dispersion in mineral oil) (4.38 mmol). The resulting mixture was stirred at room temperature for 24 h. Afterwards a 30% of the total amount of the above reagents were added and the reaction was stirred overnight. After this period, the mixture was poured into a stirred ice cold mixture of H_2O (40 mL) and CH_2Cl_2 (40 mL). The two phases were separated and the aqueous phase was extracted with CH_2Cl_2 (2 × 50 mL). The combined organic extracts were washed with saturated brine and dried over anhydrous sodium sulfate. The solvents were evaporated under reduced pressure and the residue was flashed chromatographed with petroleum ether/EtOAc 1:4 for compound **3i** and 2:3 for compound **5i**. Analytical sample for compound **3i** was prepared by recrystallization from CH_2Cl_2/petroleum ether.

4.2.3.1. 2-(3-Benzoyl-1*H*-pyrrol-1-yl)acetonitrile (3i). Yield 68%, mp 108–109 °C, IR (Nujol): 3410, 1619 cm^{-1}, ^{1}H NMR ($CDCl_3$): δ 5.10 (s, 2H, CH_2), 6.95–7.05 (m, 2H, pyrrolyl-4,5*H*), 7.40–7.80 (m, 4H, phenyl-*H* and pyrrolyl-2*H*), 7.80–8.12 (m, 2H, phenyl-*H*). Anal. Calcd for $C_{13}H_{10}N_2O(0.01CH_2Cl_2)$: C, 74.27; H, 4.79; N, 13.33. Found: C, 74.03; H, 4.78; N, 13.27.

4.2.3.2. 4-(3-Benzoyl-1*H*-pyrrol-1-yl)butanenitrile (5i). Yield 60%, yellow oil, IR (Nujol): 3517, 1637 cm^{-1}, ^{1}H NMR ($CDCl_3$): δ 2.00–2.50 (m, 4H, CH_2CH_2CN), 4.10 (t, 2H, N–CH_2), 6.64–6.89 (m, 2H, pyrrolyl-4,5*H*), 7.18–7.61 (m, 4H, phenyl-*H* and pyrrolyl-2*H*), 7.70–7.90 (m, 2H, phenyl-*H*). LC–MS calcd for $C_{15}H_{14}N_2O$: *m/z* 238.11 (100%), found: (M+23): 261.45.

4.2.4. 3-(3-Benzoyl-1*H*-pyrrol-1-yl)propanenitrile (4i)

A mixture of phenyl(1*H*-pyrrol-3-yl)methanone (0.290 g, 1.7 mmol) and 0.015 mL of Triton B (40%) was stirred under a nitrogen atmosphere. Acrylonitrile (0.12 mL, 0.096 g, 1.8 mmol) was added dropwise over 5 min. The reaction temperature was maintained below 4 °C with occasional cooling by means of an ice-water bath. After stirring at room temperature overnight, the reaction mixture was diluted with dichloromethane (20 mL), washed with water and saturated brine, and dried over anhydrous sodium sulfate and evaporated. The residue was flashed chromatographed with petroleum ether/EtOAc 2:3 to provide compound **4i** (0.229 g, yield 60%). An analytical sample was prepared by recrystallization from CH_2Cl_2/petroleum ether.Mp 69–70 °C, IR (Nujol): 3517, 1632 cm^{-1}, ^{1}H NMR ($CDCl_3$): δ 2.82 (t, 2H, CH_2CN), 4.20 (t, 2H, N-CH_2), 6.64 -6.87 (m, 2H, pyrrolyl-4,5*H*), 7.20–7.95 (m, 4H, phenyl-*H* and pyrrolyl-2*H*), 7.72–7.92 (m, 2H, phenyl-*H*). Anal. Calcd for $C_{14}H_{12}N_2O(0.001EtOAc)$: C, 74.98; H, 5.39; N, 12.49. Found: C, 74.97; H, 5.39; N, 12.49.

4.2.5. General procedure for the preparation of methyl-, ethyl- and propyl-tetrazole derivatives (3–5)

To a solution of nitriles **3i–5i** (3.33 mmol), respectively, and trimethylsilyl azide (0.88 mL, 6.66 mmol) in toluene (10 mL) was added dibutyltin oxide (0.333 mmol), and the mixture was refluxed under a nitrogen atmosphere until the nitriles were consumed (TLC analysis). The reaction mixture was concentrated in vacuo. The residue was dissolved in methanol (10 mL) and reconcentrated. The residue was treated with 10% $NaHCO_3$ (50 mL) and extracted with EtOAc (2 × 50 mL). The aqueous phase was cooled (ice bath) and acidified with 10% HCl, and extracted with EtOAc (2 × 50 mL). The combined organic extracts were washed with brine, dried over magnesium sulfate and concentrated under reduced pressure to give compounds **3**–**5**. An analytical sample of compounds **3** and **4** were prepared by recrystallization from EtOAc /petroleum ether.

4.2.5.1. (1-(2*H*-Tetrazol-5-yl)methyl)-1*H*-pyrrol-3-yl)(phenyl)-methanone (3). Yield 66%, mp 113–115 °C, IR (Nujol): 3453, 1615 cm^{-1}, ^1H NMR ($CDCl_3$/DMSO-d_6): δ 5.50 (s, 2H, C*H*$_2$), 6.57–6.99 (m, 2*H*, pyrrolyl-4,5*H*), 7.35–7.65 (m, 4H, phenyl-*H* and pyrrolyl-2*H*), 7.72–7.91 (m, 2H, phenyl-*H*). Anal. Calcd for $C_{13}H_{11}N_5O$(0.001EtOAc): C, 61.65; H, 4.38; N, 27.65. Found: C, 61.65; H, 4.38; N, 27.64.

4.2.5.2. (1-(2-(2*H*-Tetrazol-5-yl)ethyl)-1*H*-pyrrol-3-yl)(phenyl)-methanone (4). Yield 63%, mp 143–145 °C, IR (Nujol): 3432, 1605 cm^{-1}, ^1H NMR ($CDCl_3$/DMSO-d_6): δ 3.39 (t, 2H, C*H*$_2$-tetrazole), 4.41 (t, 2H, N–C*H*$_2$), 6.55–6.82 (m, 2H, pyrolyl-4,5*H*), 7.11–7.27 (m, 1H, pyrrolyl-2*H*), 7.30–7.63 (m, 3H, phenyl-*H*), 7.65–7.92 (m, 2H, phenyl-*H*). Anal. Calcd for $C_{14}H_{13}N_5O$: C, 62.91; H, 4.90; N, 26.20. Found: C, 62.86; H, 4.78; N, 26.28.

4.2.5.3. (1-(3-(2*H*-Tetrazol-5-yl)propyl)-1*H*-pyrrol-3-yl)(phenyl)-methanone (5). Yellow oil, yield 78%, IR (Nujol): 3069, 1612 cm $^{-1}$, ^1H NMR ($CDCl_3$): δ 2.31 (m, 2H, C*H*$_2$), 2.93 (t, 2H, C*H*$_2$-tetrazole), 4.03 (t, 2H, N–C*H*$_2$), 6.51–6.75 (m, 2H, pyrrolyl-4,5*H*), 7.20–7.75(m, 4H, phenyl-*H* and pyrrolyl-2*H*), 7.75–7.95 (m, 2H, phenyl-*H*), 9.95 (br s, 1*H*). LC–MS–MS calcd for $C_{15}H_{15}N_5O$: *m/z* 281.127660 (100%), found: 281.123463.

4.2.6. 5-(1H-Pyrrol-1-yl)-1H-tetrazole (6i)

2,5-Bimethoxy-tetrahydrofuran (5.36 g, 40.6 mmol) and 4-chloropyridine hydrochloride (6.79 g, 45.3 mmol) were added in a solution of 5-aminotetrazole (2.5 g, 29.4 mmol) in 1,4-dioxane (210 mL), and the mixture was refluxed under a nitrogen atmosphere for 3 h. After removal of the solvent under reduced pressure, the mixture was treated with 50 mL EtOAc and filtered. EtOAc was removed under reduced pressure from the filtrate and the residue was treated with 10% $NaHCO_3$ (20 mL) and extracted with EtOAc (2 × 50 mL). The aqueous phase was cooled (ice bath) and acidified with 10% HCl, and extracted with EtOAc (2 × 50 mL). The combined organic extracts were washed with brine, dried over anhydrous sodium sulfate, and concentrated under reduced pressure. Recrystallization from EtOAc/petroleum ether provided **6i** as a white solid. yield 63%, mp 214 °C, IR (Nujol) 3154, 2748–2347, 1627 cm^{-1}; ^1H NMR ($CDCl_3$/DMSO-d_6) δ 6.36 (s, 2H, pyrrolyl-3,4*H*), 7.47 (s, 2H, pyrrolyl-2,5*H*); Anal. Calcd for $C_5H_5N_5$: C, 44.44; H, 3.73; N, 51.83. Found: C, 44.80; H, 3.42; N, 51.65.

4.2.7. 1-(2*H*-Tetrazole-5-yl)-1*H*-pyrrol-3-yl)(phenyl)methanone (6) and 1-(2*H*-tetrazole-5-yl)-1*H*-pyrrol-2-yl)(phenyl)methanone (7)

Aluminium chloride (0.6 g, 4.5 mmol) was dissolved in the minimum amount of nitromethane (1 mL) and a suspension of **6i** (0.5 g, 3.7 mmol) in dichloromethane (25 mL) was added to the stirred mixture for 15 min at room temperature under a nitrogen atmosphere. After this period, benzoyl chloride (0.588 g, 4.2 mmol) was added and the reaction was stirred for 1.5 h under a nitrogen atmosphere. The reaction was quenched with ice and water and the product was extracted to EtOAc (70 mL). The combined organic extracts were washed with water and saturated brine, dried over anhydrous sodium sulfate, and concentrated under reduced pressure. The residue was flashed chromatographed with ether/acetic acid (0.1–0.5%) to provide compounds **6** and **7**.

4.2.7.1. 1-(2*H*-Tetrazole-5-yl)-1*H*-pyrrol-3-yl)(phenyl)methanone (6). Yield 10%, mp 189–191 °C, IR (Nujol): 3182, 2773, 1622 cm^{-1}, ^1H NMR ($CDCl_3$/DMSO-d_6): δ 6.84–7.04 (m, 1H, pyrrolyl-4*H*), 7.34–7.71 (m, 4H, phenyl-*H* and pyrrolyl-5*H*), 7.79–7.95 (m, 2H, phenyl-*H*), 7.98–8.09 (m, 1H, pyrrolyl-2*H*), 8.36 (br s, 1*H*). Anal. Calcd for $C_{12}H_9N_5O$(0.001CH_3COOH): C, 60.25; H, 3.79; N, 29.27. Found: C, 60.24; H, 3.79; N, 29.27.

4.2.7.2. 1-(2*H*-Tetrazole-5-yl)-1*H*-pyrrol-2-yl)(phenyl)methanone (7). Yield 36%, mp 103–105 °C, IR (Nujol): 3182, 2773, 1622 cm^{-1}, ^1H NMR ($CDCl_3$/DMSO-d_6): δ 6.38–6.58 (m, 1H, pyrrolyl-4H), 6.84–7.06 (m, 1H, pyrrolyl-3*H*), 7.32–7.69 (m, 4H, phenyl-*H* and pyrrolyl-5*H*), 7.78–8.08 (m, 2H, phenyl-*H*). Anal. Calcd for $C_{12}H_9N_5O$: C, 60.25; H, 3.79; N, 29.27. Found: C, 60.03; H, 3.88; N, 29.46.

4.3. In vitro assays

4.3.1. In vitro aldose reductase enzyme assay

The target compounds **1**–**7** as well as the reference compound sorbinil ($C_{11}H_9FN_2O_3$, Phizer, Inc., Central Research Division, Groton, CT, USA) were dissolved in aqueous solution of $NaHCO_3$. Lenses were quickly removed from Fischer-344 rats of both sexes following euthanasia and homogenized. The experiments conform to the law for the protection of experimental animals (Republic of Greece) and are registered at the Veterinary Administration of the Republic of Greece. The enzyme preparation and assay were performed as previously described.[35,9] All compounds except **3**–**5** were tested at five concentrations, the log (dose)–response curves were then constructed from the inhibitory data, and the IC_{50} values were calculated by least-square analysis of the linear portion of the log (dose) versus response curves ($0.952 < r^2 < 0.994$). The experiments were performed in triplicate.

4.3.2. In vitro aldehyde reductase enzyme assay

ALR1 from rat kidney was partially purified according to the reported procedure of Constantino et al.[16] as follows: kidneys were quickly removed from rats following euthanasia and homogenized in a knife homogenizer followed by processing in a glass homogenizer with a teflon pestle in 3 vol of 10 mM sodium phosphate buffer, pH 7.2, containing 0.25 M sucrose, 2.0 mM EDTA dipotassium salt, and 2.5 mM β-mercaptoethanol. The homogenate was centrifuged at 10,000 rpm at 0–4 °C for 20 min and the supernatant was subjected to ammonium sulfate fractional precipitation at 40%, 50%, and 75% salt saturation. The pellet obtained from the last step, possessing ALR1 activity, was redissolved in 10 mM sodium phosphate buffer, pH 7.2, containing 2.0 mM EDTA dipotassium salt and 2.0 mM β-mercaptoethanol to achieve total protein concentration of approx. 20 mg/mL. DEAE DE 52 resin was added to the solution (33 mg/mL) and after gentle mixing for 15 min removed by centrifugation. The supernatant containing ALR1 was then stored in smaller aliquots at −80 °C. No appreciable contamination by ALR2 in ALR1 preparations was detected since no activity in terms of NADPH consumption was observed in the presence of glucose substrate up to 150 mM.

4.3.3. DPPH assay

To investigate the antiradical activity of the title compounds **6**, **7** and **I** in a homogeneous system, a method based on the scavenging of the stable free radical DPPH was used.[14] Compounds **6**, **7** and **I** and the reference compound 6-hydroxy-2,5,7,8-chroman-2-carboxylic acid (trolox) were dissolved in 1 mL of absolute ethanol (0.4–0.025 mM) and added to 1 mL solution of DPPH in absolute ethanol (0.4 mM) to give final concentrations of 0.2–0.0125 mM and 0.2 mM for the tested compounds and DPPH, respectively. The continual absorbance decrease of the ethanol solution of the stable free radical at 517 nm, in the presence of the tested compounds, was measured. The experiments were performed in triplicate.

4.3.4. Liposome preparation, incubation and LOOH determination

The experimental protocol is based on a previously described methodology.[14] A suspension of unilamellar L-α-phosphatidylcholine dioleoyl (C18:1,[*cis*]-9; DOPC; 99% grade) liposomes (1 mM) in phosphate buffer (20 mL, 20 mM, pH 7.4) was prepared. The liposomes (final concentration 0.8 mM DOPC) were incubated in the presence of different concentrations of compound **4 (10–300** μM) with the water-soluble initiator AAPH (final concentration 10 mM) at 50 °C for 80 min. Aliquots (1 mL) of the incubation mixtures were extracted with 2 mL portions of an ice-cold mixture of $CHCl_3$/MeOH (2:1, v/v) containing 2,6-di-*tert*-butyl-*p*-cresol (BHT) (0.05%). The lipid hydroperoxide content was determined by the thiocyanate method by sequentially adding the $CHCl_3$/MeOH (2:1, v/v) mixture (1.4 mL) and the thiocyanate reagent (0.1 mL).[36] The thiocyanate reagent was prepared by mixing equivalent volumes of a methanolic solution of KSCN (3%) and a ferrous ammonium sulfate solution (45 mM in 0.2 mM HCl). After the mixture had been left at ambient temperature for at least 5 min, the absorbance at 500 nm was recorded. The lipid peroxide value was determined using a calibration curve prepared with standard cumene hydroperoxide. The experiment was performed in triplicate.

4.4. Computational methods

The molecules **3**, **6**, and **7** were constructed using SYBYL molecular modeling package[37], and their energies were minimized using the Powell method with a convergent criterion provided by the Tripos force field.[38] The X-ray structure of human aldose reductase holoenzyme (PDB 1US0) was used in our docking calculations after deletion of the inhibitor IDD 594 from the PDB file, obtained from the Brookhaven Protein Data Bank.[39]

Docking calculations were performed with GLUE program implemented in the GRID package (www.moldiscovery.com).[40] GLUE[41] is a docking procedure aimed at detecting energetically favourable binding modes of a ligand with respect to the protein active site using the GRID force field.[42] The protein cavity is mapped using several GRID runs: a set of different probes is used to mimic all chemical groups present in the ligand and the resulting maps are encoded into compact files which store the interaction energies. Afterwards, an iterative procedure identifies all the ways in which four atoms of the ligand could bind to the target, by pairing every atom to the 'nearest' MIF used. Hydrophobic and polar atoms of the ligand for which several conformers are quickly produced are fitted over their corresponding energy maps, giving rise to sometimes millions of ligand orientations, which are temporarily stored. Then, many orientations are quickly eliminated due to redundancy and steric hindrance constraints. Redundancy occurs whenever two or more orientations are close enough to each other, that is, the rmsd calculated over their 3D structures is lower than 2.0 Å; therefore, they are grouped and one orientation represents the entire group. Conversely, steric hindrance occurs whenever part of the ligand clashes into the binding site: in this case, the clashing part is accommodated along the site if possible; otherwise, the orientation is excluded. Indeed, this refinement allows only reliable orientations to be processed in the next step: each orientation is optimized within the cavity by means of successive torsions and translations. These are driven by the ligand-target interaction energy computed by the GRID force field: each little movement is followed by an energy reassessment according to the GRID standard equation applied over the whole ligand and the active site:

$$\mathrm{EGRID} = \mathrm{ELJ} + \mathrm{EEL} + \mathrm{EHB} + \mathrm{EENTROPY}$$

The optimized orientations represent possible binding modes of the ligand within the site. The interaction energy between the entire ligand and the protein binding site is calculated by using the GLUE equation, which provides an energy scoring function (EGLUE) composed by four contributions: ESR = steric repulsion energy, EES = electrostatic energy, ERHB = hydrogen bonding charge reinforcement, and EDRY = hydrophobic energy.

$$\mathrm{EGLUE} = \mathrm{ESR} + \mathrm{EES} + \mathrm{ERHB} + \mathrm{EDRY}$$

The final output of the docking procedure is a set of solutions ranked according to the corresponding scoring function values, each defined by the 3D coordinates of its atoms and expressed as a PDB file. PyMol molecular graphics system was used in order to visualize the results of the docking.[43]

Acknowledgements

Many thanks to Professor J. Stephanidou-Stephanatou, Department of Organic Chemistry, School of Chemistry, Aristotle University of Thessaloniki, Professor K. Fytianos, Enviromental Pollution Control Laboratory, School of Chemistry, Aristotle University of Thessaloniki for their important contribution on the reception of LC/MS and LC–MS/MS spectra, respectively and Professor Anna Tsantili-Kakoulidou, School of Pharmacy, University of Athens for the permission to use the Pallas program. The authors are also grateful to Professor Gabriele Cruciani (Laboratory for Chemometrics, School of Chemistry, University of Perugia, Italy) for kindly providing us the GRID package, to Assoc. Professor Thomas Mavromoustakos (Department of Chemistry, University of Athens) for kindly allowing us access to the SYBYL molecular modelling package.

References and notes

1. Venkat Narayan, K. M. *Clin. Diabetes* **2005**, *23*, 51.
2. Boel, E.; Selmer, J.; Flodgaard, H. J.; Jensen, T. *J. Diabetes Complications* **1995**, *9*, 104.
3. Constantino, L.; Rastelli, G.; Vianello, P.; Cignarella, G.; Barlocco, D. *Inc. Med. Res. Rev*. In *Vol. 19*; John Willey & Sons, 1999.
4. Kangas, T.; Aro, S.; Koivisto, V. A.; Salinto, M.; Laakso, M.; Reunanen, A. *Diabetes Care* **1996**, *19*, 494.
5. Parving, H. H. *Diabetologia* **1997**, *40*, B9.
6. Sheet, M. J.; King, G. L. *J. Am. Med. Assoc.* **2002**, *288*, 2579.
7. Ramirez, M. A.; Borja, N. L. *Pharmacotherapy* **2008**, *28*, 646.
8. Alexiou, P.; Pegklidou, K.; Chatzopoulou, M.; Nicolaou, I.; Demopoulos, V. *Curr. Med. Chem.* **2009**, *16*, 734.
9. Nicolaou, I.; Demopoulos, V. *J. Med. Chem.* **2003**, *46*, 417.
10. Perrier, L.; Bourrie, M., et al *J. Pharmacol. Exp. Ther.* **1994**, *271*, 91.
11. Hansch, C.; Leo, A. In *Exploring QSAR. Fundamentals and Applications in Chemistry and Biology*; Heller, S. R., Ed.; ACS Professional Reference Book: American Chemical Society: Washington, DC, 1995; p 520.
12. Barski, O. A.; Gabbay, K. H.; Grimshaw, C. E.; Bohren, K. M. *Biochemistry* **1995**, *34*, 11264.
13. Rees-Milton, K. J.; Jia, Z.; Green, N. C.; Bhatia, M.; El-Kabbani, O.; Flynn, T. G. *Arch. Biochem. Biophys.* **1998**, *355*, 137.
14. Alexiou, P.; Nicolaou, I.; Stefek, M.; Kristl, A.; Demopoulos, V. *J. Bioorg. Med. Chem.* **2008**, *16*(7), 3926.
15. Mylari, B. L.; Armento, S. J.; Beebe, D. A.; Conn, E. L.; Coutcher, J. B.; Dina, M. S.; O'Gorman, M. T.; Linhares, M. C.; Martin, W. H.; Oates, P. J.; Tess, D. A.; Withbroe, G. J.; Zembrowski, W. J. *J. Med. Chem.* **2005**, *48*, 6326.

16. Constantino, L.; Rastelli, G.; Gamberini, M. C.; Vinson, J. A.; Bose, P.; Iannone, A.; Staffieri, M.; Antolini, L.; Del Corso, A.; Mura, U.; Albasini, A. *J. Med. Chem.* **1999**, *42*, 1881.
17. Demopoulos, V. J.; Rekka, E. *J. Pharm. Sci.* **1995**, *84*, 79.
18. Meinwald, J.; Meinwald, Y. C. *J. Am. Chem. Soc.* **1966**, *88*, 1305.
19. Wittenberger, S. J.; Donner, B. G. *J. Org. Chem.* **1993**, *58*, 4139.
20. Nicolaou, I.; Demopoulos, V. J. *J. Heterocycl. Chem.* **1998**, *35*, 1345.
21. Gui, T.; Tanimoto, T.; Kokai, Y.; Nishimura, C. *Eur. J. Biochem.* **1995**, *227*, 448.
22. Del Corso, A.; Constantino, L.; Rastelli, G.; Buono, F.; Mura, U. *Exp. Eye Res.* **2000**, *71*, 515.
23. Kador, P. F.; Sharpless, N. E. *Mol. Pharmacol.* **1983**, *24*, 521.
24. Brubaker, A. N.; De Ruiter, J.; Whitmer, W. L. *J. Med. Chem.* **1986**, *29*, 1094.
25. Sun, W. S.; Park, Y. S.; Yoo, J.; Park, K. D.; Kim, S. H.; Kim, J.-H.; Park, H.-J. *J. Med. Chem.* **2003**, *46*, 5619.
26. Koukoulitsa, C.; Zika, C.; Geromichalos, G. D.; Demopoulos, V. J.; Skaltsa, H. *Bioorg. Med. Chem.* **2006**, *14*, 1653.
27. Djoubissie, P.-O.; Snirc, V.; Sotnikova, R.; Zurova, J.; Kyselova, Z.; Skalska, S.; Gajdosik, A.; Javorkova, V.; VlkoviCova, J.; Vrbjar, N.; Stefek, M. *Gen. Physiol. Biophys.* **2006**, *25*, 415.
28. Stefek, M.; Snirc, V.; Djoubissie, P.-O.; Majekova, M.; Demopoulos, V. J.; Rackova, L.; Bezakova, Z.; Karasu, C.; Carbone, V.; El-Kabbani, O. *Bioorg. Med. Chem.* **2008**, *16*, 4908.
29. El-Kabbani, O.; Podjarny, A. *Cell. Mol. Life Sci.* **2007**, *64*, 1970.
30. Blois, M. S. *Nature* **1958**, *181*, 1199.
31. Rackova, L.; Stefek, M.; Majekova, M. *Redox Rep.* **2002**, *7*, 207.
32. Lipinski, C. A.; Lombardo, F.; Dominy, B. W.; Freeney, P. *J. Adv. Drug Deliv. Rev.* **2001**, *46*, 3.
33. Remko, M.; Swart, M.; Bickelhaupt, F. M. *Bioorg. Med. Chem.* **2006**, *14*, 1715.
34. Ertl, P.; Rohde, B.; Selzer, P. *J. Med. Chem.* **2000**, *43*, 3714.
35. Nicolaou, I.; Zika, C.; Demopoulos, V. J. *J. Med. Chem.* **2004**, *47*, 2706.
36. Mihaljevic, B.; Katusin-Razem, B.; Razem, D. *Free Radical Biol. Med.* **1996**, *21*, 53.
37. SYBYL, version 8.0, TRIPOS Associates Inc., S. Louis MO.
38. Vinter, J. G.; Davis, A.; Saunders, M. R. *J. Comput. Aided Mol. Des.* **1987**, *1*, 31–51.
39. RCSB Protein Data Bank, operated by the Research Collaboratory for Structural Bioinformatics.
40. GRID version 22, Molecular Discovery Ltd, 4. Chandos Street, W1A 3BQ, London, United Kingdom.
41. Carosati, E.; Sciabola, S.; Cruciani, G. *J. Med. Chem.* **2004**, *47*, 5114.
42. Goodford, P. J. *J. Med. Chem.* **1985**, *28*, 849.
43. DeLano, W.L., The PyMOL Molecular Graphics System DeLano Scientific, San Carlos, CA, USA, 2002.